

# Thermal Error Modelling of a CNC Machine Tool Feed Drive System using FEA Method

Ayman Abuaniza  
Mechanical Engineering Department,  
Almerighb university  
Alkhmos, Libya

Naeem S Mian  
Centre for Precision Technologies  
School of Computing and Engineering,  
University of Huddersfield  
Huddersfield, UK

Simon Fletcher  
Centre for Precision Technologies  
School of Computing and Engineering,  
University of Huddersfield  
Huddersfield, UK

Andrew P Longstaff  
Centre for Precision Technologies  
School of Computing and Engineering,  
University of Huddersfield  
Huddersfield, UK

**Abstract**— Recirculating ball screw systems are commonly used in machine tools and are one of the major heat sources which cause considerable thermal drift in CNC machine tools. Finite Element Analysis (FEA) method has been used successfully in the past to model the thermal characteristics of machine tools with promising results. Since FEA predictions are highly dependent on the efficacy of numerical parameters including the surrounding Boundary Conditions (BC), this study emphasises on an efficient modelling method to obtain optimised numerical parameters for acquiring a qualitative response from the feed drive system model. This study was performed on a medium size Vertical Machining Centre (VMC) feed drive system in which two parameter identification methods have been employed; the general prediction method based on formulae provided by OEMs, and the energy balance method. The parameters obtained from both methods were applied to the FEA model of the machine feed drive system and validated against experimental results. Correlation with which was increased from 70 % to 80 % using the energy balance method.

**Keywords**—FEA; Energy balance method; formula method; Feed drive system; VMC.

## I. INTRODUCTION

It is well known that heat generated in ball screw feed drive systems can cause significant positioning errors on machine tools [1]. There are a number of feed drive thermal models to investigate the thermal responses of machine tool, such as mechanical design modification, multiple regression, genius education algorithm, applying pretension on feed drive system, and using FEA modelling [2-6]. Xu et al. [2, 5] conducted an experimental study to control heat in a high precision ball screw drive system named “centre hole cooling”. They found that the centre hole cooling brings temperature-equilibrium state faster to the ball screw system. The air/liquid cooling system is applied to the whole ball screw shaft to increase the positioning accuracy directly since it causes a uniform heat power distribution.

Yang et al. [3] developed an FEM-based thermal model to resolve the temperature change and distribution that was causing the thermal deformation of the ball screw. Simulations were carried out to appraise the effects of cooling enhancement on thermal deformations by replacing a solid ball screw shaft with a hollow shaft. The deformations, however, obtained from the FEM predictions and the experimental results were in good agreement. These methods add cost, are time consuming and may not be retrofit table onto existing machines.

Huang [4] analysed the thermal displacement of a ball screw feed drive system using MRA method. Three temperature increases locations at front bearing, nut and back bearing were selected as independent variables of the analysis model and recorded by thermal couples. The estimated and experimental results were compared and exposed that 73–83 % thermal errors can be minimised. Yun et al. [6] used the genius education algorithm and modified lumped capacitance method to analyse the thermal error of the ball screw system. Their results indicate that the thermal error was also reduced to less than 15 %. Although, these methods gave acceptable results, longer experimental regimes were required to collect large data sets in order to identify factors for building these models which therefore entails unwanted longer machine downtimes [4, 6, 7].

A common method used by machine tool builders to decrease the effect of ball screw expansion is by applying pre-tension (stretch) to the ball screw to absorb some of feed drive expansion and rise the axial stiffness of the screw [8]. Gim et al. [9] reported that it is required to apply tension on the ball screw that suits changes of its temperature. Fletcher et al. [8] proved experimentally that applying pretension can reduce thermal error in the ball screw, but only by a relatively small amount and also that the thermal datum becomes less predictable compare to a fixed-floating arrangement. The experiments further revealed that the application of much higher levels of pre-tension than normally used by OEMs did not incur a significant benefit towards the reduction of thermal error.

## Acknowledgements

The authors gratefully acknowledge the Libyan culture affairs in London, the UK’s Engineering and Physical Sciences Research Council (EPSRC) funding of the EPSRC Centre for Innovative Manufacturing in Advanced Metrology (Grant Ref.: EP/I033424/1). The authors wish to thank all the partners of the consortium.

Due to the fact that thermal behaviour of machine tools is complicated, the finite element method has been widely used in such circumstances [10-12]. The drawback of this method has been the use of assumed parameters to simplify the calculations for heat transfer coefficients.

The objective of this paper is to compare two principal methods that can be used to compute the heat power of the various heat sources. In the first method, the heat power was calculated using the standard formulae based on established literature or provided by the manufacturers. In the second method, the heat power was obtained by experiments, in which a thermal imaging camera was used to measure the temperature rise in the ball screw periodically. Furthermore, a laser interferometer was used to periodically measure the thermal error accordingly. The heat power of heat sources were calculated using the heat transfer balance equations. This method has been successfully applied to a machine tool spindle by Mian [11, 13] but not a feed-drive system where the heat sources are generally more difficult to measure using thermal imaging. The convective coefficients were computed analytically for both low and rapid table feeds. It would be desirable to use purely analytically determined values to reduce the requirement for further on-machine testing. The heat power obtained from both methods were then applied to the FEA model of the ball screw and compared for their effectiveness. To the authors' knowledge, there is no single comparison study of heat power calculations methods has been done for machine tools.

## II. EXPERIMENTAL SET-UP

The ball screw of a medium VMC horizontal axis was chosen as a typical representative low cost feed drive system, a schematic of which is shown in Figure 1. It consists of the ball screw shaft, ball screw nut and bed saddle. The ball screw shaft is axially constrained and radially supported by a pair of single row angular contact ball bearings at the driven end and the other end is only radially supported. The bearing is mounted in housings located inside the saddle. An AC motor is used to drive this system. The specifications of the ball screw feed drive system are listed in Table 1.

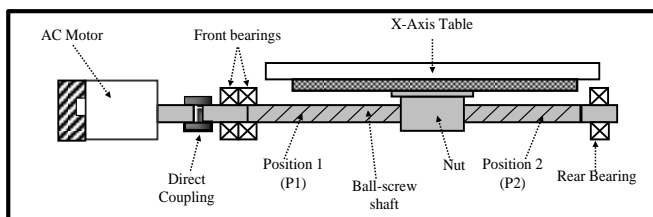


Figure 1: Schematic of the ball screw feed drive system

Table 1: Specification of ball screw feed drive system

Ball screw specifications	
Parameters	Value
Maximum speed	267 rpm
Axis stroke	500 mm
Nut length	100 mm
Preload of nut	3000±200 N
Nut type	Single

Nominal outer diameter of ball screw shaft	20 mm
Lead	10 mm
Mass of bed saddle	122 Kg
Mass of table	105 Kg
Bearing type	7204B (NSK)

Throughout the experiment, the temperature change and thermal deformation were recorded by the infrared (IR) camera and laser interferometer, respectively. Figure 2 shows the actual set up of the experiment. The initial temperature for the feed drive system was measured to be 23 °C.

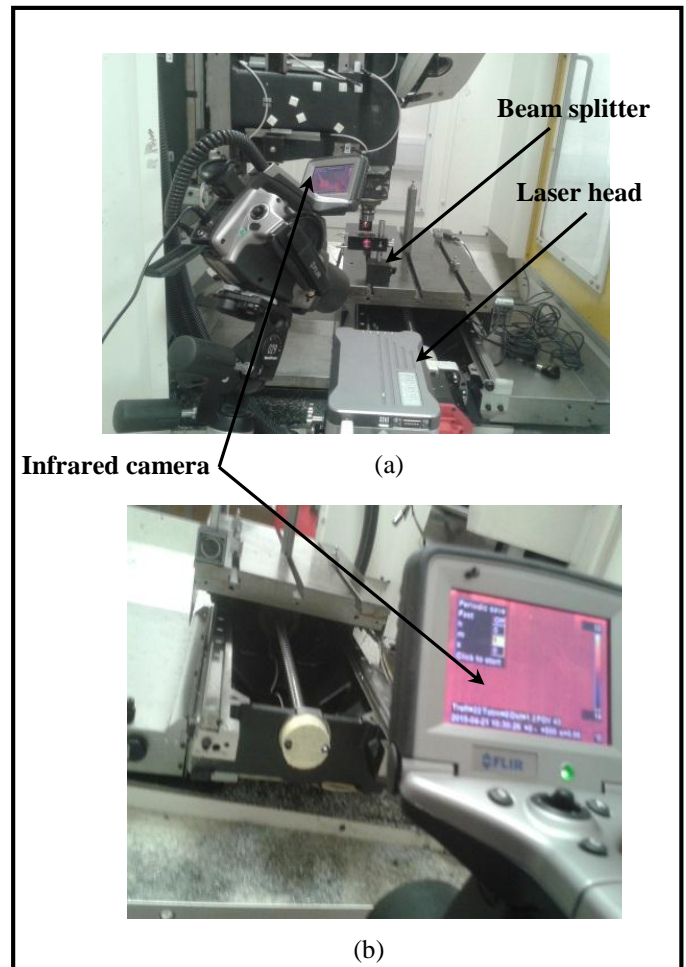


Figure 2: Experimental set up: (a) Front view. (b) Rear view.

The table movement was along the x-axis with a full traverse of 500 mm. The temperatures were measured at equal intervals of 10 sec, see Figure 3. According to ISO 230-part 3 [14] two target positions should be selected close to the end point of axes travel, due to which, the start and the end positions of the X axis traverse were selected for the measurement of thermal error. During the heating cycle of 2 hours, the table was run rapidly ten times at the feed rate of 21 m/min which is approximately 70 % of the maximum feed rate [14]. At the end of each rapid cycle, the table was traversed at a slow feed rate of 2 m/min with two stop positions P1 (0 mm) and P2 (500 mm), during which, the displacement data was recorded. See Figure 1 for the positions P1 and P2.

The cooling cycle lasted for 1 hour, during which, the table was rested for 60 s before it moved to the measuring positions P1 and P2 to record the displacement data, see Figure 4.

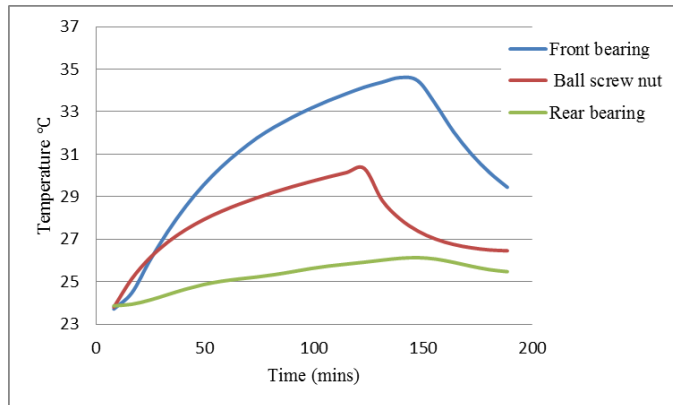


Figure 3 Temperature gradient of ball screw nut, front and rear bearings

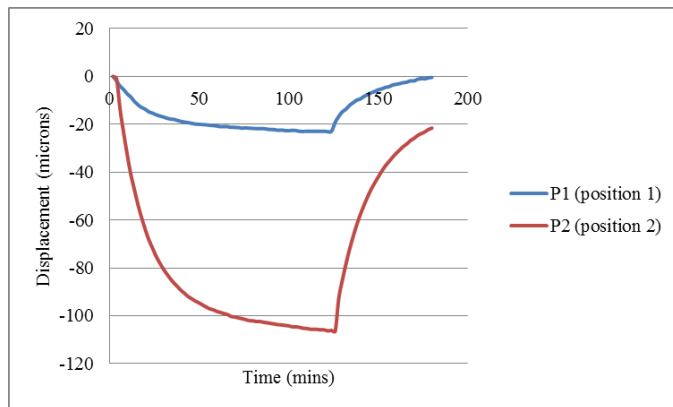


Figure 4 Displacement of feed drive system at two points

### III. THERMAL MODEL

FEA model of the ball screw feed drive system was created using the SolidWorks 2013, see Simplifications are made to the model to reduce the computation time. These include removal of small holes, small chamfers, small fillets, T-slots, bolts and bolt holes. In order to obtain high calculating precision, more mesh elements were assigned to elements representing heat power sources and adjacent areas [15]. Total of 40147 nodes and 24926 contact elements were selected for the FEA model, see Figure 7.

Thermal contact resistance (TCR) between bolted joints was considered in the FEA model. The TCR is mainly determined by contact pressure, contact medium, material properties on both sides of the joint, and roughness of the surfaces. The clamping force of the oiled ball screw nut and bearings, which tighten by screws of M12, is 80 KN [16], due to which, the TCR of 0.0004 ( $m^2 \cdot ^\circ C/W$ ) was applied, as explained by Mian & et al. [13]. The TCR between the ball screw nut and ball screw shaft has different magnitude due to complicated surface contact.

#### A. TCR of ball screw nut and ball screw shaft.

Using the temperature sensors in the hollow ball screw, heat transfer from the nut to the screw has been measured. The nut was rapidly heated at one position on the screw then, for cooling, moved to a part of the screw not yet affected by the heat. At this position, with the nut stationary, any heat entering the screw must have transferred by conduction from the nut. The measured temperatures were then used to calculate a heat transfer coefficient.

Figure 5 shows the temperature of the nut and the screw shaft under the nut (the length of the contact area of the nut completely covers 2 temperature sensors in the hollow ball screw) during the transition from heating to cooling. The slope of the curve calculated from H and L equates to the heat transfer. For the recorded data, the heat transfer value is  $66 W/m^2 \cdot ^\circ C$  when the contact area between the nut and the screw is estimated to be  $0.017 m^2$ .

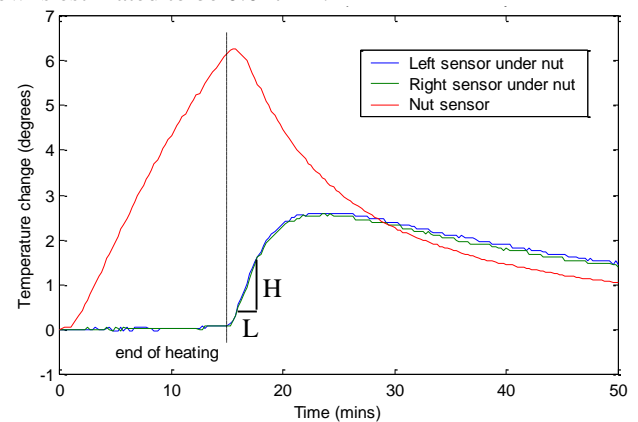


Figure 5 Graph showing heat conduction from nut to screw sections under nut

Throughout the feed drive thermal error modelling experiment, the table was moved 500 mm. Therefore, the contact area is changed to  $0.0314 m^2$  and TCR between the ball screw nut and ball screw shaft is  $0.028 m^2 \cdot ^\circ C/W$ . These figures of TCR were used in the FEA model at the relevant joints, i.e. joints between the ball screw nut and ball screw shaft.

The following assumptions are made in order to simplify the thermal model:

- The screw shaft is simplified to be a solid cylinder [17].
- The radiation term can be neglected as the temperatures involved are relatively low.
- During the measurement runs, the convective heat transfer coefficient was assumed to be steady during the cooling phase since the table movement was very slow.
- The TCR for the support bearing and the ball nut interfaces was the same

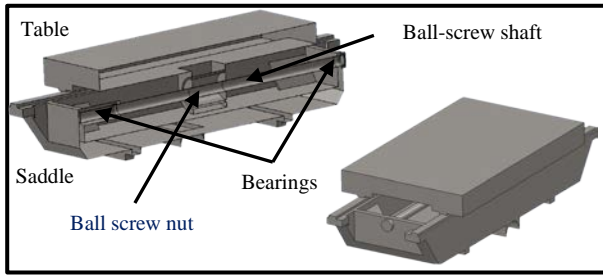


Figure 6: Solid model of the ball screw system

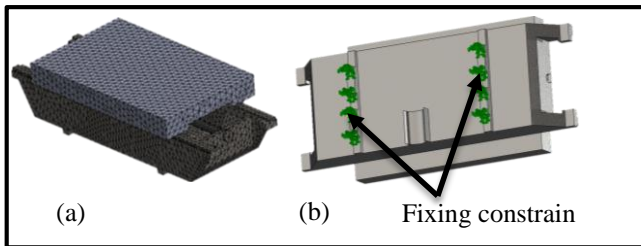


Figure 7: (a) Finite element analysis the ball screw system model; (b) Fixing constrain position

#### IV. COMPUTATION OF THE CONVECTION COEFFICIENT OF HEAT TRANSFER

As the ball screw rotates, the resulting air flow means that forced convection must be considered for accurate modelling. Forced convection coefficient can be computed by heat transfer equations of air flow along a horizontal cylinder [18].

$$\bar{N}_{ud} = CRe_D^m Pr^{1/3} \quad (1)$$

Where  $\bar{N}_{ud}$  is the average Nusselt number, C and m are the constants,  $Re_D$  is the Reynolds number, Pr is the Prandtl number.

$$\bar{N}_{ud} = \frac{\bar{h} d}{k} \quad (2)$$

Where  $\bar{h}$  is the average convection coefficient ( $W/m^2 \cdot ^\circ C$ ), d is the ball screw diameter (m), k is the thermal conductivity ( $W/m \cdot ^\circ C$ ). The Reynolds number  $Re_D$  is calculated using:

$$Re = \frac{ud}{\nu} \quad (3)$$

Where d is the ball screw shaft diameter (m),  $\nu$  is the kinematic viscosity ( $\frac{m^2}{s}$ ), u is the velocity of the flow ( $\frac{m}{s}$ ). The velocity of the flow can be calculated from the following equation

$$u = \frac{\pi dn}{60} \quad (4)$$

Where d and n are the ball screw shaft diameter (m) and its speed (rpm) respectively.

At normal temperatures, the Prandtl number of the air is 0.701, the kinematic viscosity of the air is  $16 \cdot 10^{-6} m^2/s$ ,  $m=0.5$ ,  $C= 0.683$  [18] (m and C are the constants in equation (1)). Using these equations, the convection coefficient was calculated to be  $12 W/m^2 \cdot ^\circ C$  which was applied throughout the rapid table feed rate. In contrast, since the table movement during the measurement runs is very slow, the airflow was assumed to be close to natural, therefore, the natural convective coefficient of  $6 W/m^2 \cdot ^\circ C$  determined by Mian et al [13] was applied to the table.

#### V. HEAT GENERATION

There are three heat sources in this feed drive system;

- Heat generated between the nut and screw shaft.
- Heat generated by support bearings due to the friction between the balls and races.
- Heat generated by the guideway.

In this study two different methods are used to obtain the heat power which later on is compared. The first one is based on the established literature and it will be referred to as the “formula method”. The second method is based on the energy balance method and as such will be labelled as “energy balance method”.

##### A. Formula method

##### 1) The heat generation due to friction between ball screw shaft and nut

The rolling (or running) torque required to overcome friction in the ball screw and nut system depends on a number of factors such as size, lubrication, types of seals and preload. To maintain accuracy and high rigidity, suitable preload must be applied to the ball screw nut system. Consequently, additional heat will be generated due to friction caused by preload. Tenjitus et al. [19], reported that heat generation, which can be named thermal load, can be calculated by the following equation.

$$P = 0.12\pi nM \quad (4)$$

Where P is the heating power (W), n is the rotational speed (rpm), M is the total frictional torque (N·m), which entails friction torque  $M_d$  and resistance torque  $M_{pl}$ .

$$M_d = T_d(1 - \epsilon) \quad (5)$$

$$M_{pl} = \frac{F_p L}{2\pi \epsilon} (1 - \epsilon^2) \quad (6)$$

Where  $T_d$  is the driving torque,  $F_p$  is the preload and  $\epsilon$  is the efficiency of a ball screw which equals 0.95 [19].

$$T_d = \frac{FL}{2\pi \epsilon} \quad (8)$$

Where F is the axial load and L is the lead of ball screw.

The heat power generated due to friction between the ball screw nut and ball screw shaft found 25 W. There can be uncertainties in formulae method calculation which eventually lead to the formula method giving no accurate results. The uncertainties were in machine component measurements and their specifications due to the fact that the manufacturer's drawings and specifications were not available.

##### 2) Bearing heat generation

As with the ball screw, heat generated in the angular contact rolling element bearing due to friction is influenced by speed, preload, and lubricant and can be calculated by the following equation [20].

$$H_b = 1.047 \cdot 10^{-4} \cdot n \cdot M_t \quad (9)$$

Where n is the rotational speed,  $M_t$  is the total torque of the bearing. The total torque is the sum of the load torque and viscous friction torque.



$$M_t = M_1 + M_v \quad (10)$$

Where  $M_1$  is the load dependent friction torque, which can be calculated from the following equation:

$$M_1 = f_1 p_1 d_m (Nmm) \quad (11)$$

Where  $f_1$  is a factor depending on bearing design,  $p_1$  is the relative bearing preload and  $d_m$  is the mean diameter of the bearing. For angular contact bearings:

$$f_1 = 0.001 \left(\frac{p_0}{c_0}\right)^{0.33} \quad (7)$$

$$p_1 = 1.4f_a - 0.1f_r \quad (8)$$

$M_v$  Viscous friction torque and can be empirically expressed as [17]

$$M_v = 10^{-7} f_0 (\vartheta_0 n)^{2/3} d_m^3 \quad (9)$$

If  $\vartheta_0 n > 2000$

$$M_v = 160 * 10^{-7} f_0 d_m^3 \quad (10)$$

If  $\vartheta_0 n < 2000$

Where  $f_0$  is a factor that depends on bearing type and lubrication type.

The specification of bearings can be found in

**Table 2.**

Table 2: Bearing specification

Bearing	Front/rear
Contact angle	40°
Inner diameter	20 mm
Outer diameter	47 mm
Mean diameter	33.5 mm
Width	14 mm
Lubrication mode	Oil spot

The heat power generated due to friction between the front bearings, rear bearing and the ball screw shaft found 4.5 W and 2 W respectively. More heat generated by front bearings as they provide support axially and radially while rear bearing provide only radially support. These calculations might have some uncertainties as the bearings are not visible and manufacture's drawing not available.

### 3) Heat generated by the guideway

The guideways are also one of the possible heat sources in the machine tool, particularly for high speed machining and where hydrostatic systems are used. In this case, for common rolling element bearings, heat generation of the guideways can be calculated by the following equation [17].

$$q_g = \mu FV \quad (11)$$

Where  $q_g$  is the heat power,  $\mu$  is the friction coefficient,  $F$  is the normal load,  $V$  is the velocity of table. From equation (16), it was found that the heat power on each side of table slides is 1.25 W for velocity of 21 m/min and a friction coefficient of 0.12 [17]. There is strong possibility of calculation uncertainties also in heat power generated by guideways as there could be rolling elements which was not included in the CAD model as they are not visible and manufacturing drawing not available. The temperature of the guideways was measured using the thermal imaging (see Figure 8) which showed no significant increase in temperature. This could be due to the fact that medium VMC has small sized guideways ( $\approx 20 \text{ mm}^2$ ) and the highest feed rate of this machine is still relatively low and therefore not sufficient to generate heat flow across guideways as compared to other machine tools with high speed systems.

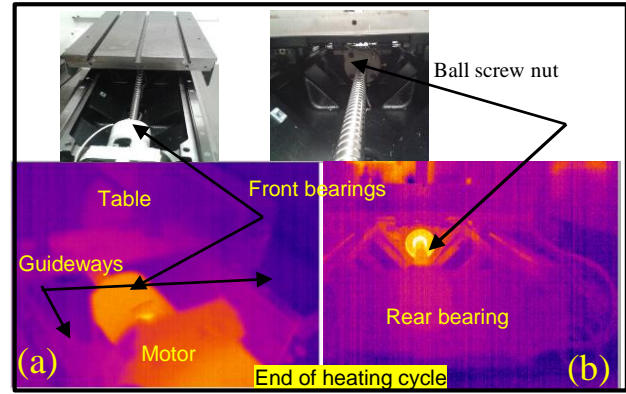


Figure 8: Main structure and thermal image of ball screw feed drive system: (a) Front view (b) Rear view

### B. Energy Balance method

Heat power of all sources in the ball screw feed drive system can be calculated using equation (17) based on temperature data from a thermal imaging sequence and estimates of the convective heat transfer coefficient. The heat sources, which are front bearing, rear bearing and ball screw nut, of the feed drive system were imaged periodically (every 10 s) utilising the thermal imaging camera. This is more often than is typically required to track temperature change but this oversampling was useful to mitigate the fact that the table moves forward and backward, making it difficult to have all the thermal images of the heat sources. However, it was possible to have reasonable temperature gradient of the heat sources despite some missing data.

$$Q = \frac{mc_p(T_2 - T_1)}{dt} + hA(T_{surface} - T_{air}) \quad (12)$$

Where  $Q$  is the heat power (W),  $m$  is the mass (kg),  $(T_2 - T_1)$  is the surface temperature difference ( $^{\circ}\text{C}$ ),  $T_{surface}$  is the surface temperature ( $^{\circ}\text{C}$ ),  $T_{air}$  is the air temperature ( $^{\circ}\text{C}$ ),  $dt$  is the time intervals (s),  $C_p$  is the specific heat ( $\frac{\text{J}}{\text{kg}\cdot^{\circ}\text{C}}$ ),  $h$  is the heat transfer convective coefficient ( $\frac{\text{W}}{\text{m}^2\cdot^{\circ}\text{C}}$ ),  $A$  is the area ( $\text{m}^2$ ). The obtained heat power parameters are shown in Table 3

Table 3: Heat power of the significant heat sources

Heat sources	Heat power (W) formula method	Heat power (W) balance method
Front bearing	4.5	7
Rear bearing	2	4
Ball screw nut	25	27.5
Guideways of table	1.25	Negligible

From Table 3, one can observe the difference in heat power obtained using both methods. When a machine tool is brand new, the formula method and the balance method may be more likely to give similar results of heat power since the machine tool is in its ideal condition and the components are closer to specification. However, in the case of a used machine tool, the energy balance method is probably more accurate as the machine elements efficiency decreases due to many reasons such as wear, misalignments and low efficiency clamping system force. The medium VMC under consideration is at least five years old therefore, in its current condition, the balance method would be ideal to obtain more

reliable and accurate behaviour of the temperature and displacement compared to the formulae method, shown in Figure 14, Figure 15, Figure 16 and Figure 17. This is validated in the following section.

### VI. THERMAL CHARACTERISTICS

The ball screw feed drive system is made from steel. The material properties applied to the ball screw model are shown in

Table 4.

Table 4: Material properties of Steel

Material	Steel
Density Kg/m <sup>3</sup>	7800
Specific heat ( $\frac{j}{kg \cdot ^\circ C}$ )	500
Thermal conductivity (W/m.k)	30
Thermal expansion coefficient (1/°C)	1.2*10 <sup>-5</sup>

The FEA model of the feed drive was simulated while the table is stationary which is different from the actual experiment. In order to address this simplification and reduce the effect on the simulation results, the total heat power, which is generated due to friction between balls and ball screw shaft at one side and the other side between balls and body of ball screw nut, see Figure 9, was applied to balls representative body which attached to ball screw nut body at one side and the other side ball screw shaft. This can simulate the actual heat transfer in the experiment as the heat conducts to the body of ball screw nut and ball screw shaft.

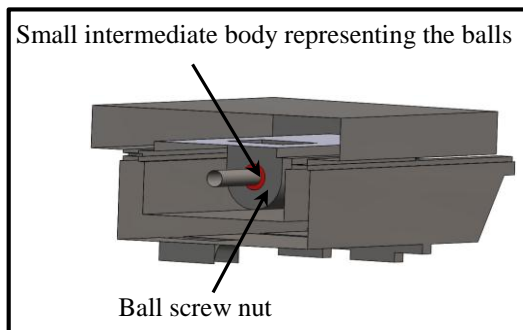


Figure 9 Ball screw nut details

Furthermore, in the experiment due to the movement of the ball screw nut, the temperature gradient of the ball screw shaft is uniform; therefore, the total expansion of it is the total uniform expansion of its elements. This is not the case in simulation as the table is stationary. This problem was tackled by applying the total heat power to the balls representative body which make the elements under and adjacent to balls representative body expand more than the actual ones and the other element expand less. However, the total expansion of simulated ball screw shaft should be equal to the actual total expansion.

This can be validated by simulating a shaft which has same dimension and specification of the ball screw shaft of the feed drive system. The shaft was divided in to 6 parts in order to apply heat power to be applied to some of these parts. The TCR at parts connection was considered to be zero to represent heat flow in one part shaft, see Figure 10.

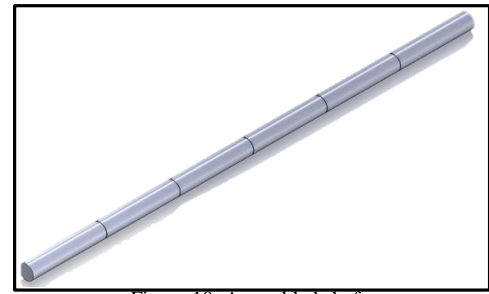


Figure 10 Assembled shaft

The gradient of shaft temperature was simulated twice: the first one, heat power of 2 W was applied to all parts in order to have uniform temperature gradient and the second simulation done by applying heat power of 6 W to two middle parts. The second simulation is similar to feed drive system simulation, see Figure 11.

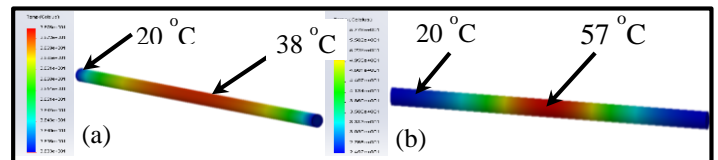


Figure 11 Assembled shaft simulation: (a) heat power applied to all of it (b) heat power applied to two middle parts

The correlation of the simulated stabilization period data with the experimental stabilization period data was obtained. One side of the assembled shaft was constrained to be fixed. The simulated displacement data was probed from a node positioned at the end of the assembled shaft. Figure 12 shows the total displacements, which are probed at the free end of the shaft, are almost the same.

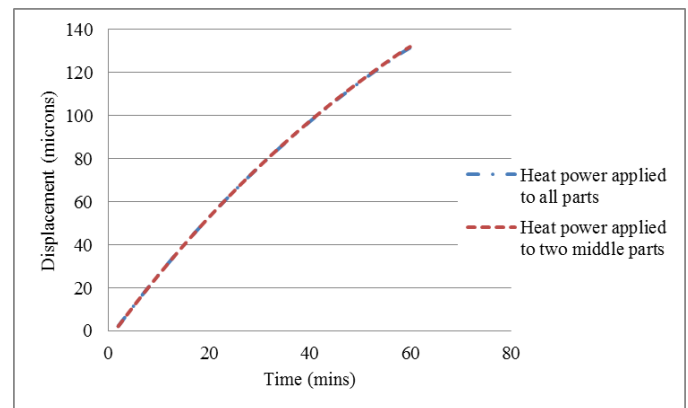


Figure 12 Simulation of ball screw shaft using different heat power distribution

### VII. THERMAL SIMULATION OF THE FEED DRIVE SYSTEM

Transient studies for each simulation were conducted for the same time as the experiments, (3 hours: 2 h heating and 1 h cooling). The numerical parameters calculated for the heat sources shown in Table 3 and boundary conditions were applied to the respective elements in the FEA model. These include convective heat transfer coefficients applied to the table, ambient conditions and fixed geometry constraints to the saddle to treat it as constrain, as depicted in Figure 7.

The temperature gradient simulation of the feed drive is shown Figure 13. There is a small temperature increase in the table due to the effects of heat generated at the ball screw nut and front bearings. The correlation between simulated and experimental data was good (85 %).

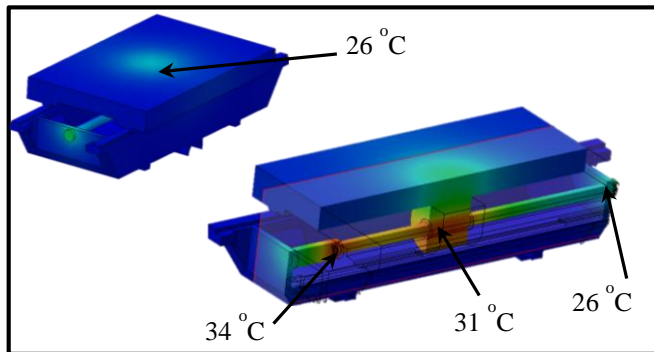


Figure 13: The temperature distribution of feed drive system

Figure 14, Figure 15, show the high temperature gradient of ball screw nut and front bearings while small temperature increase of the rear bearing as depicted in Figure 16. This is expected because the rear bearing is smaller (only one race) and only supports the ball screw shaft radially which reduces the amount of load applied on it compared to front bearings. Simulated temperature data was compared with experimental data using both methods.

The first stage is to correlate the simulated stabilization period data with the experimental stabilization period data. The saddle bottom was constrained to be fixed. The simulated data was measured from nodes positioned at the actual displacement sensor positions utilised to observe the displacement of the feed drive system as discussed in the experiment set up section earlier. Figure 17 show simulated and experimental displacement data in the X-axis using energy balance and formulae methods.

It can be observed that the simulation results from the energy balance method correlate more closely with the experimental data than the results from the formulae method. The remaining thermal error in X-axis at position 2 (P2) is approximately 30  $\mu\text{m}$  using the formulae method while it can be decreased to less than 18  $\mu\text{m}$  using the energy balance method from 106  $\mu\text{m}$ . At position 1 (p1) the thermal error was reduced to approximately 6  $\mu\text{m}$  using formulae method whereas it was decreased to 4  $\mu\text{m}$  using the energy balance method from 20  $\mu\text{m}$ , Figure 18.

It can be noticed that more thermal error at the P2 than P1 as P2 is near to fixed end of the ball screw shaft and it is the start point of table movement while the p1 is near to the free end point and the end point of the table movement.

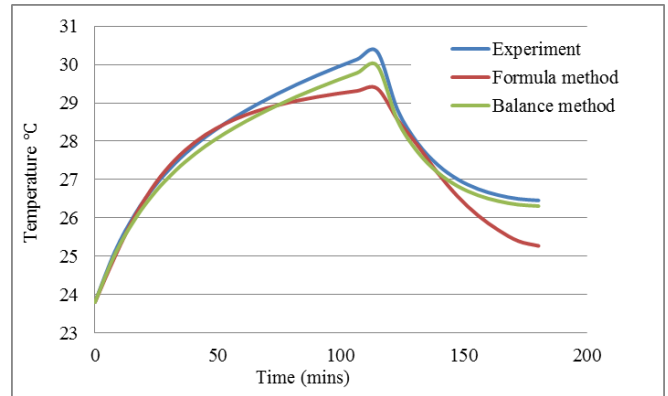


Figure 14: Experimental and simulated ball screw nut temperature comparison

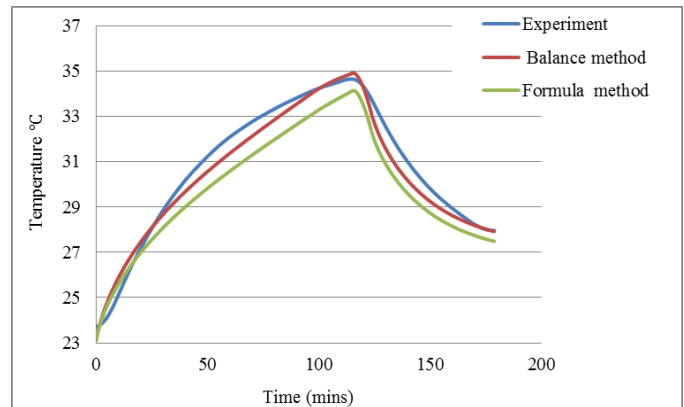


Figure 15 Experimental and simulated front bearing temperature comparison

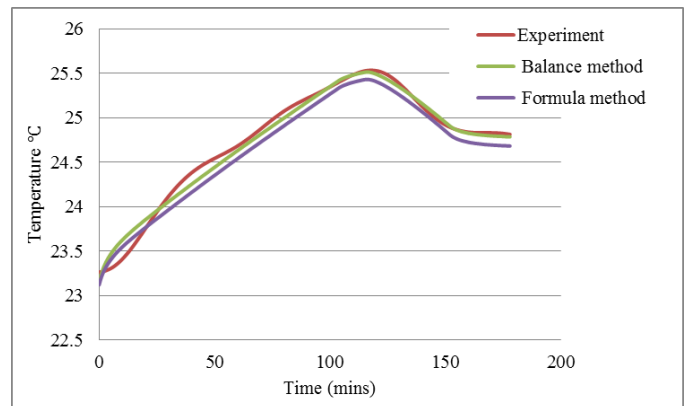


Figure 16: Experimental and simulated rear bearing temperature comparison

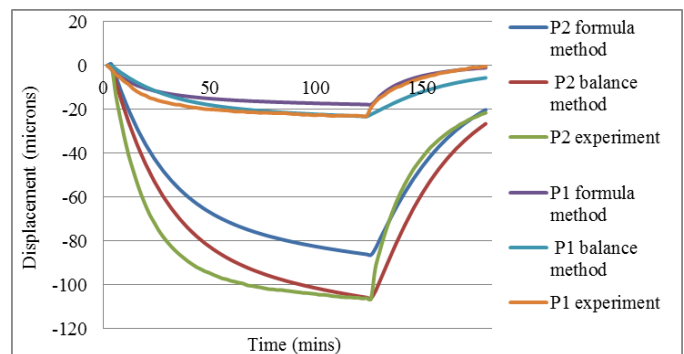


Figure 17: Experimental and simulated displacement comparison at two positions

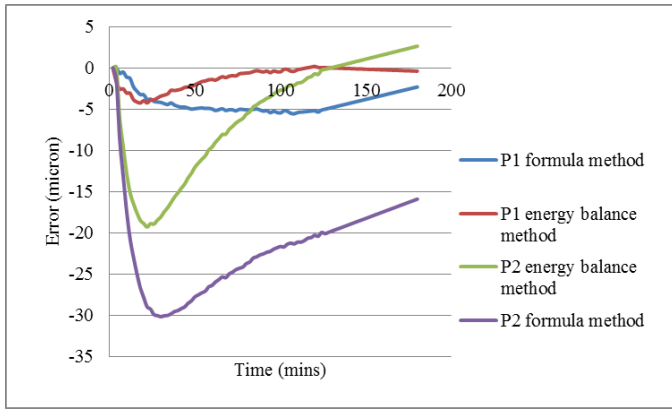


Figure 18 Residual error of feed drive system

In order to further validate the performance of FEA model on another set of data, a much long-term and more random duty cycle was conducted on the same machine as follows: The duty cycle took 6 h and 15 minutes, 1.5 h heating cycles with feed rate of 21 m/min, it followed by 1 hour cooling down, then 2 hours heating up at feed rate of 15 m/min and 1 h and 45 minutes cooling down at the end. During the experiment, the ball screw nut and bearings temperature gradient was recorded periodically by thermal imaging camera and the thermal errors were measured by the laser interferometer.

In order to validate the FEA model on the experimental results from a complex duty cycle, the same heat power values listed in Table 3 was utilised at the same duty cycle test time. Figure 19, Figure 20, Figure 21 and Figure 22 show duty cycle of experimental and simulated data of temperature gradient and thermal errors profiles.

Although the displacement results are the most important from a performance perspective, the following temperature comparisons are also included for information on how well the extended simulation matches the experiment. **Figure 19**

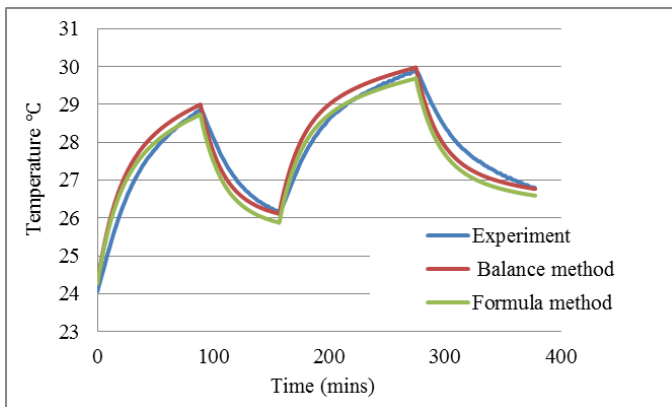


Figure 19 Duty cycle test profile of experimental and simulated ball screw nut temperature comparison

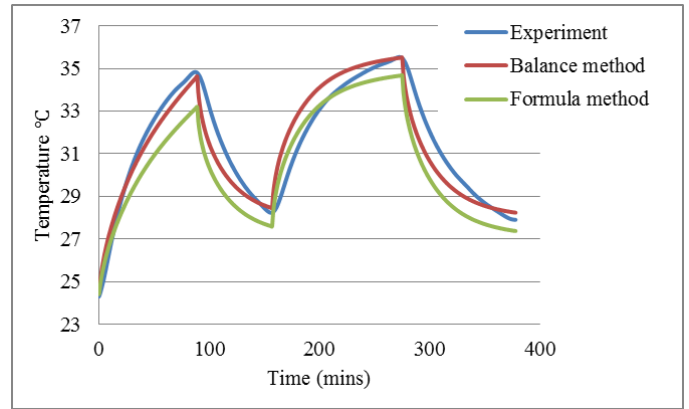


Figure 20 Duty cycle test profile of experimental and simulated front bearings temperature comparison

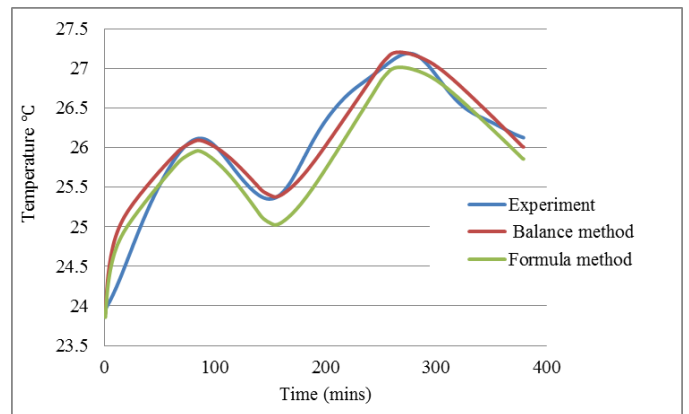


Figure 21 Duty cycle test profile of experimental and simulated rear bearing temperature comparison

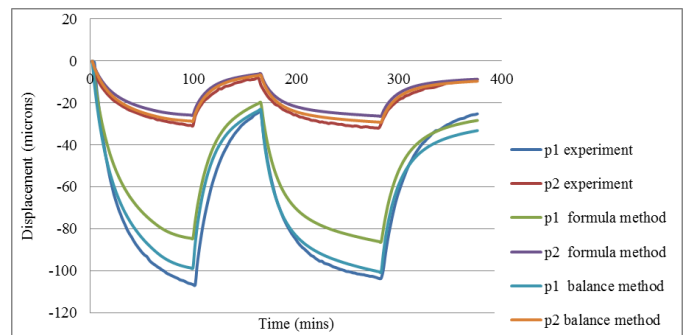


Figure 22 Duty cycle test profile of experimental and simulated displacement comparison at two positions

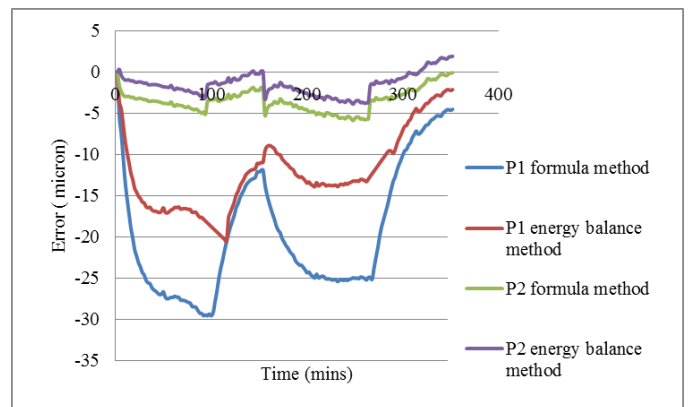


Figure 23 Residual error of feed drive system



From the duty cycle test results, it can be again noticed that simulation results from the energy balance method agreed well with the experimental data than the results from the formulae method.

The duty cycle test also reveals that the remaining thermal error in X axis at position 2 (P2) is approximately 30  $\mu\text{m}$  using the formulae method while it reduced to 20  $\mu\text{m}$  using the energy balance method from 106  $\mu\text{m}$ . At position 1 (p1) the thermal error was reduced to approximately 6  $\mu\text{m}$  using formulae method whereas it was decreased to 4  $\mu\text{m}$  using the energy balance method from 20  $\mu\text{m}$ , see Figure 23.

### VIII. CONCLUSIONS

Many small to medium sized or relatively low value machine tools use rotary encoders for positioning therefore the ball screw is part of the position feedback loop. Errors of a feed drive system are primarily caused by the thermal deformation of a ball screw shaft as it is heated through use. In this paper, thermal error of feed drive system in a medium VMC machine tool were studied and analysed experimentally and the effects of internally generated heat on the positioning error of a ball screw feed drive system were predicted offline using the FEA model. To ensure accurate FEA predictions, the boundary conditions such as the heat transfer convective coefficients were calculated analytically. The core of this research was to calculate the heat power of the feed drive system heat sources using two different methodologies; the formula; and the energy balance and compare them for their effectiveness. The correlations between the experimental and FEA simulated results revealed 70 % for the formulae method and 80 % for the balance method. In terms of the residual error, the comparison revealed the error of 30  $\mu\text{m}$  using the formulae method and 18  $\mu\text{m}$  using the energy balance method. The improvements in the FEA results are evident that the energy balance method has provided optimised parameters representative of the real state of the machine. Another important highlight is that the energy balance method is an easy to implement and a quicker method to apply for obtaining the thermal behaviour for any feed drive system. Moreover, since the machine under consideration was not new, the energy balance method has been proved to be more realistic and effective for assessing the current thermal status of the feed drive system.

### REFERENCES

- [1] J. Bryan, *International status of thermal error research*, . Annals of the CIRP, vol 39(2): p. pp 573.1990.
- [2] Z. Xu, X. Liu, H. Kim, J. Shin, and S. Lyu, *Thermal error forecast and performance evaluation for an air-cooling ball screw system*. International Journal of Machine Tools and Manufacture, vol 51(7): p. 605. 2011.
- [3] A. Yang, S. Cai, S. Hsieh, T. Kuo, C. Wang, W. Wu, W. Hsieh, and Y. Hwang, *Thermal deformation estimation for a hollow ball screw feed drive system*. Paper presented in Proceedings of the world congress on engineering Vol. 3, London, U.K. 2013.
- [4] Huang, S.-C. *Analysis of a model to forecast thermal deformation of ball screw feed drive systems*. International Journal of Machine Tools and Manufacture, vol 35(8): p. 1099. 1995.
- [5] Z.-Z. Xu, X.-J. Liu, C.-H. Choi, and S.-K. Lyu, *A study on improvement of ball screw system positioning error with liquid-cooling*. International Journal of Precision Engineering and Manufacturing, vol 13(12): p. 2173. 2012.
- [6] W. S. Yun, S. K. Kim, and D. W. Cho, *Thermal error analysis for a CNC lathe feed drive system*. International Journal of Machine Tools and Manufacture, vol 39(7): p. 1087. 1999.
- [7] S. Kim and D. Cho, *Real-time estimation of temperature distribution in a ball-screw system*. International Journal of Machine Tools and Manufacture, vol 37(4): p. 451. 1997.
- [8] S. Fletcher and D. G. Ford, *Measuring and modelling heat transfer and thermal errors on a ballscrew feed drive system*, in Lamdamap, Uk, 2003.
- [9] T. Gim, J.-y. Ha, J.-y. Lee, C.-h. Lee, and T.-j. Ko, *Ball screw as thermal error compensator*, in Proceedings form ASPE Annual Meeting 2001.
- [10] H. Su, L. Lu, Y. Liang, Q. Zhang, Y. Sun, and H. Liu, *Finite element fractal method for thermal comprehensive analysis of machine tools*. The International Journal of Advanced Manufacturing Technology, p. 1. 2014.
- [11] N. S. Mian, S. Fletcher, A. P. Longstaff, and A. Myers, *Efficient estimation by FEA of machine tool distortion due to environmental temperature perturbations*. Precision Engineering, vol 37: p. 372. 2012.
- [12] J. Mayr, J. Jedrzejewski, E. Uhlmann, M. Alkan Donmez, W. Knapp, F. Härtig, K. Wendt, T. Moriwaki, P. Shore, and R. Schmitt, *Thermal issues in machine tools*. CIRP Annals-Manufacturing Technology, vol 61(2): p. 771. 2012.
- [13] N. S. Mian, S. Fletcher, A. P. Longstaff, and A. Myers, *Efficient thermal error prediction in a machine tool using finite element analysis*. Measurement Science and Technology, vol 22(8): p. 85. 2011.
- [14] ISO 230-3, *Test code for machine tools- part 3: Detemination of thermal effects*, . 2007.
- [15] X. Min, J. Shuyun, and C. Ying, *An improved thermal model for machine tool bearings*. International Journal of Machine Tools and Manufacture, vol 47(1): p. 53. 2007.
- [16] ISO 898-1, *Mechanical properties of fasteners made of carbon steel and alloy steel Part 1: Bolts, screws and studs with specified property classes – Coarse thread and fine pitch thread*. 2013.
- [17] X. Min and S. Jiang, *A thermal model of a ball screw feed drive system for a machine tool*. Proceedings of the Institution of Mechanical Engineers, Part C: Journal of Mechanical Engineering Science, vol 225(1): p. 186. 2011.
- [18] F. P. Incropera, D. P. Dewitt, T. L. Bergman, and A. S. Lavine, *Introduction to Heat Transfer*, John Wiley & Sons, United States of America, 2007.
- [19] W. Tenjitus, *Solution for heating of ball screw and environmental engineering*. Key Compon. CNC Mach. Tool, vol 3: p. 65. 2004.
- [20] Z. Haitao, Y. Jianguo, and S. Jinhua, *Simulation of thermal behavior of a CNC machine tool spindle*. International Journal of Machine Tools and Manufacture, vol 47(6): p. 1003. 2007.